ELSEVIER

Journal of Photochemistry and Photobiology A: Chemistry 90 (1995) 1–9

Journal of PHOTOCHEMISTRY AND PHOTOBIOLOGY A:CHEMISTRY

A kinetic investigation of Sr[5s6s($^1S_0$)] in energy pooling from Sr[5s5p(^3P_J)] studied by time-resolved atomic emission following pulsed dye-laser excitation

S. Antrobus, D. Husain *, Jie Lei

Department of Physical Chemistry, University of Cambridge, Lensfield Road, Cambridge CB2 1EW, UK

Received 16 January 1995; accepted 21 March 1995

Abstract

We present a kinetic study of Sr[5s6s($^1S_0$)] generated by energy pooling arising from self-annihilation of Sr[5s5p(^3P_J)]. Sr[5s5p($^3P_1$)] was produced by pulsed dye-laser excitation at $\lambda = 689.3$ nm (Sr[5s5p($^3P_1$)] ← Sr[5s^2($^1S_0$)]) of strontium vapour at elevated temperatures (750–890 K) in the presence of excess helium buffer gas. Following rapid Boltzmann equilibration within the 5s5p(^3P_J) spin–orbit manifold, time-resolved emission was monitored at $\lambda = 1124.1$ nm (Sr[5s6s($^1S_0$)] → Sr[5s5p($^1P_1$)]) using signal averaging methods. To our knowledge, this constitutes the first direct observation of this time-resolved emission, which has become feasible through the commercial development (Hamamatsu) of a new long-wavelength photomultiplier tube (350–1200 nm) based on an Ag–O–Cs photocathode, whose operation and application in the present system are described in some detail. Subsequent time-resolved emission at $\lambda = 460.7$ nm (Sr[5s5p($^1P_1$)] → Sr[5s^2($^1S_0$)]) is thus seen to result from "cascading fluorescence" as originally proposed by Gallagher and coworkers. First-order decay coefficients, characterized across the above temperature range for Sr[5s6s($^1S_0$)], Sr[5s5p($^1P_1$)] and Sr[5s5p(^3P_J)], are shown to be in the ratio of 2:2:1 in accord with self-annihilation, energy pooling emission and cascading fluorescence. Integrated atomic emission intensity profiles for the transitions at $\lambda = 1124.1$ nm and 460.7 nm, coupled with optical and electronic sensitivity calibrations, yield an estimate of the Einstein coefficient for the $\lambda = 1124.1$ nm transition based on the above mechanism. Finally, the present optical system, using the new photomultiplier tube with the associated optics and gating circuitry, is seen to provide a basis for studying low-lying electronically excited states above the ground state (more than approximately 1.03 eV), particularly Ba[6s5d($^3D_{1,2,3}$)] and Ba[6s5d($^1D_2$)] by time-resolved emission.

Keywords: Energy pooling; Time-resolved atomic emission; Pulsed dye-laser excitation

1. Introduction

Energy pooling of electronically excited alkaline earth atoms in low-lying metastable states has been widely studied following laser excitation of ground state ns^2($^1S_0$) atomic vapours of these metals. These excited states are sufficiently metastable to be investigated conveniently in the time domain [1–4] and under single-collision conditions [5], but are characterized by Einstein coefficients of such magnitude to yield relatively high densities on laser excitation. Emission from higher lying atomic states may be observed following the bimolecular collision processes between these metastable states. These "energy pooled states" are often characterized by short radiative lifetimes and may be investigated by time-resolved emission. The time profiles of both the energy "store" and "pool" states are then characterized in the kinetic investigations. Energy pooling investigations from electronically excited atomic strontium alone in the presence of a noble gas have been limited. Kelley et al. [6] have observed emission from Sr[5s6s($^3S_1$)] (3.600 eV [7]) and Sr[5s5p($^1P_1$)] (2.690 eV [7]) following laser excitation of Sr(5^3P_1), and have characterized the absolute rate constants into the energy pooled 6^3S_1 and 6^1S_0 states following pulsed dye-laser generation of Sr(5^3P_J) and Sr(5^3P_J) + Sr(5^3P_J) self-annihilation [8]. Husain and Roberts [9] have presented a detailed kinetic study of energy pooling from both the low-lying, optically metastable states of atomic strontium, Sr[5s5p(^3P_J)] and Sr[5s4d($^1D_2$)], 1.807 and 2.261 eV respectively above the 5s^2($^1S_0$) ground state [7]. For excitation of Sr(5^3P_J), emission from pooled states was essentially restricted to Sr(6^3S_1) and Sr(5^1P_1). Emission from Sr[5s4d($^1D_2$)] was very weak and subject to overlapping from neighbouring transitions [9]. Very recently, we have

* Corresponding author.

1010-6030/95/$09.50
DI 1010-6030(95)04083-8

reported time-resolved emission for a larger number of energy pooled states, namely Sr[5s5p($^1P_1$)], Sr[5s6s($^3S_1$)], Sr[4d5p($^3F_{2,3,4}$)], Sr[4d5p($^1D_2$)], Sr[5s6p($^3P_{1,2}$)], Sr[5s5d($^3D_2$)] and Sr[5p^2($^3P_2$)], derived from Sr[5s5p(^3P_J)] following pulsed dye-laser generation of Sr[5s5p($^3P_1$)] from the ground state atomic vapour [10]. Many of these states lie significantly higher in energy above two Sr(5^3P_J) atoms, namely 3.614 eV, the highest being Sr[5p^2($^3P_2$)] (4.423 eV [7,10]). Quantitative characterization of integrated atomic emission intensities has established that the energy pooled states arise from bimolecular self-annihilation of Sr(5^3P_J) and that the relative yields into the pooled states are consistent with the Boltzmann population into those states where the pooling processes are endothermic.

An important aspect of energy pooling from Sr(5^3P_J), not experimentally accessible by direct spectroscopic investigation hitherto, has been the proposal of Kelley et al. [8] that emission at $\lambda = 460.7$ nm (Sr[5s5p($^1P_1$)] → Sr[5s^2($^1S_0$)]) is not direct energy pooling fluorescence but "cascading fluorescence". These workers suggest that the 5s5p($^1P_1$) state is populated by the long-wavelength emission Sr[5s6s($^1S_0$)] → Sr[5s5p($^1P_1$)] + $h\nu$ ($\lambda = 1124.1$ nm) and that the 5s6s($^1S_0$) state is, in fact, the pooled state [8]. Production of this pooled state is endothermic to the extent of approximately 1500 cm^{-1} from two Sr(5^3P_J) atoms [7]. On this basis, we have employed the integrated emission at $\lambda = 460.7$ nm to calculate the relative yield into Sr[5s6s($^1S_0$)] [10]. However, it must be stressed that time-resolved emission at $\lambda = 1124.1$ nm has not been observed hitherto for the technical reason that even long-wavelength photomultiplier tubes are not normally sensitive at this wavelength. In this paper, we describe the observation of this emission from Sr[5s6s($^1S_0$)] in the time domain from energy pooling from Sr(5^3P_J). This has become feasible using a new photomultiplier tube that has recently become available. The circuitry, gating system, optical sensitivity calibration and operation of this device with a new monochromator–grating combination are described in this paper. Time profiles for emission from Sr[5s5p($^3P_1$)], Sr[5s5p($^1P_1$)] and Sr[5s6s($^1S_0$)] are reported, the latter being shown to arise kinetically from Sr(5^3P_J) + Sr(5^3P_J) self-annihilation, supporting the proposal of Kelley et al. [8]. The characterization of integrated atomic emission profiles, including that at $\lambda = 1124.1$ nm, is used to estimate the Einstein coefficient for this long-wavelength emission. Finally, the implications for studying time-resolved emission for low- lying atomic states using this new photomultiplier system, including Ba[6s5d($^3D_{1,2,3}$)] and Ba[6s5d($^1D_2$)] within the context of electronically excited alkaline earth atoms, are briefly considered.

2. Experimental details

The general experimental arrangement for monitoring atomic resonance fluorescence, energy pooling emission and

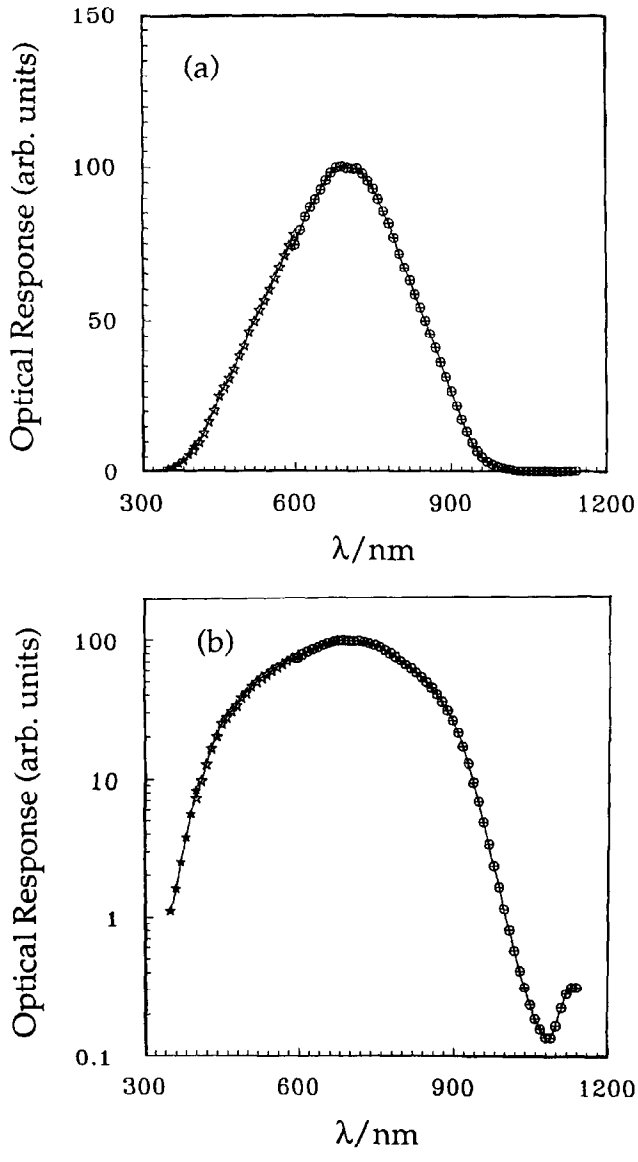

Fig. 1. Calibration of the optical response of the monochromator (GM 100), grating (GM 100-5) and long-wavelength response photomultiplier tube (R632, Hamamatsu, S1 response) ((a) direct output; (b) logarithmic display) employed in the investigation of the energy pooling of Sr(5^3P_J) generated by the pulsed dye-laser excitation of strontium vapour at $\lambda = 689.3$ nm (Sr[5s5p($^3P_1$)] ← Sr[5s^2($^1S_0$)]) at elevated temperatures: ★, no filter; ☆, clear glass; ⊕ orange filter.

cascading emission in the time domain was similar to that described in recent investigations on chemical reactions of Sr(5^3P_J) [11,12], but with significant modification to the optical detection system. Sr[5s5p($^3P_1$)] was thus generated by the Nd:YAG-pumped pulsed dye-laser excitation (10 Hz) (J.K. Lasers, System 2000) of strontium vapour at elevated temperatures [13] at $\lambda = 689.3$ nm (Sr[5s5p($^3P_1$)] ← Sr[5s^2($^1S_0$)]) in the presence of excess helium buffer gas in a slow flow system, kinetically equivalent to a static system. In contrast with our previous system employed for studies of the chemical reaction of Sr(5^3P_J) [11,12] and energy pooling [10], a further high-throughput compact monochromator (Spiers Robertson GM 100; aperture ratio f 4.7; fixed slits,

0.5 mm) was used. This included a grating with optical sensitivity at long wavelength (Spiers Robertson GM 100-5; range, 350–1100 nm; 590 grooves mm^{-1}; blaze, 500 nm). The further effect of the blaze wavelength will be noted presently.

The specifications of the new IR-sensitive photomultiplier tube employed in this investigation (Hamamatsu R632 - S1 response) are given in the commercial literature, but appropriate aspects that particularly affect the present measurements are presented here. This is a 12-dynode device with a photocathode material of Ag–O–Cs and a sensitivity range of approximately 400–1200 nm, although the commercial response curve is only presented up to 1100 nm. The wavelength response shows a bimodal distribution, with maxima at about 310 and 800 nm and a trough at 450 nm. The overall sensitivity is relatively low, the quantum efficiency being little more than 1% at 310 nm and 0.1% at 1000 nm. Nevertheless, the operational wavelength range is large, permitting optical measurements in this range with constant light gathering power. The gain (G) of the tube can sensibly be described by the form $\ln G = 8.48 \ln V(\mathrm{V}) - 47.28$ ($\gamma = 0.998$) from the commercial gain characteristic. The photomultiplier gating circuitry to eliminate the effect of scattered light from the laser initiation pulse was similar to that employed in previous investigations on $Sr(5^3P_J)$ [10–12]. In this case, a reverse pulse of 100 V of varied duration was applied across the fifth and seventh dynodes of the photomultiplier chain, during which the laser pulse was applied, yielding an attenuation of approximately 100 : 1.

The wavelength response of the photomultiplier–grating combination was calibrated using a quartz halogen lamp and a spectral radiometer (International Light Inc., USA, IL783) as employed on earlier optical systems for studying $Sr(5^3P_J)$ [10–12]. The resulting calibration curve is shown in Fig. 1(a). Hence the double maxima in the wavelength response of the photomultiplier tube coupled with the blaze of the grating (see earlier) yields a curve with a single maximum. The caption in Fig. 1 indicates the use of standard filters employed as part of the spectral radiometer. The response at, for example, $\lambda = 1100$ nm is not zero but about 0.3 on the arbitrary scale given in Fig. 1 and the response is approximately flat at this value to $\lambda = 1200$ nm. The logarithmic display given in Fig. 1(b) emphasizes the optical response at long wavelength. Small variations in the region of 1100 nm (approximately 0.2–0.3) are, of course, exaggerated. This low long-wavelength response is offset in the measurements by the increase in gain of the photomultiplier tube with voltage (see earlier) which, necessarily involving scatter from noise in the tube, is significantly reduced by signal averaging (see later, this section).

Following the earlier procedure [10–12], digitized data capture of complete profiles was employed in contrast with

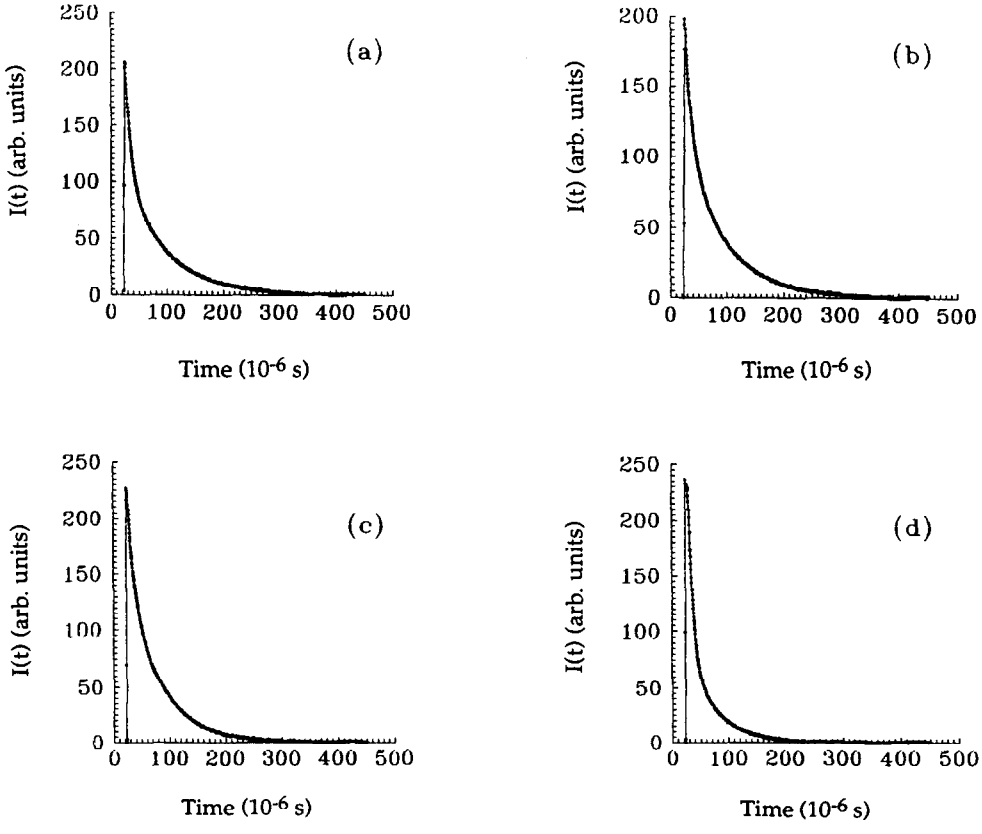

Fig. 2. Examples of the digitized output showing the decay of the time-resolved atomic fluorescence emission $I(t)$ at $\lambda = 689.3$ nm ($Sr[5s6s(^3S_1)] \rightarrow Sr[5s5p(^3P_0)]$) following the pulsed dye-laser excitation of strontium vapour at the resonance wavelength in the presence of helium buffer gas ($p_{He} = 80$ Torr, 9.1×10^{17} atoms cm^{-3} at 850 K) at elevated temperatures. T (K): (a) 850; (b) 830; (c) 790; (d) 750.

the earlier use of boxcar integration. Thus decay profiles were captured with a double-channel transient digitizer (Digital Storage Adapter, Thurlby DSA 524) interfaced to a computer. Decay profiles (255) were captured and averaged as were 255 background profiles before transfer and subtraction for computerized analysis. Measurements of the integrated atomic intensities were calculated from the recorded decay profiles coupled with calibration of the response of the optical system and the photomultiplier gain characteristic. The materials (Sr, He) were employed essentially as described in the previous investigations on energy pooling on atomic strontium [9,10].

3. Results and discussion

Fig. 2 gives examples of the digitized output, indicating the decay of the time-resolved emission $\lambda = 689.3$ nm ($Sr[5s5p(^3P_1)] \rightarrow Sr[5s^2(^1S_0)] + h\nu$) following laser excitation at this resonance wavelength at different temperatures. The kinetic study of energy pooling, of course, requires the quantitative characterization of the kinetic behaviour of the ^3P_J store state as well as the pooled states. The range of temperatures given in Fig. 2 is employed here in order to obtain a variation in the first-order decay coefficient k' for the decay of $Sr(5^3P_J)$ via the subsequent variation in the "escape factor" (g), studied in radiation trapping in this type of system [14], for different atomic densities of $Sr(5^1S_0)$ and different ambient temperatures (see later). Fig. 3 gives the computerized fitting of the digitized output in Fig. 2, indicating the first-order decay of the time-resolved emission $\lambda = 689.3$ nm ($Sr[5s5p(^3P_1)] \rightarrow Sr[5s^2(^1S_0)] + h\nu$) at times greater than approximately 50 μs for all the decays. We may readily show from approximate calculations of the laser linewidth and energy output at the resonance wavelength, together with estimates of the lineshape at $\lambda = 689.3$ nm, that it is possible in these measurements to generate densities of $Sr(5^3P_1)$ which are significant compared with those of the $Sr(5^1S_0)$ ground state. This yields a kinetic term for the removal of $Sr(5^3P_J)$ involving $[Sr(5^3P_J)]^2$ which is significant at earlier times and causes departures from linearity in the first-order kinetic plots as shown in Fig. 3.

Under the first-order conditions we may write

$$[Sr(5^3P_J)]_t = [Sr(5^3P_J)]_{t=0} \exp(-k't) \quad (1)$$

The overall first-order decay coefficient k' may then be expressed in the form [10–13]

$$k' = k_{em} + \beta/p_{He} + \Sigma k_Q[Q] \quad (2)$$

where k_{em} represents the first-order loss due to radiative decay from $Sr(5^3P_1)$, where the $^3P_0$ and $^3P_2$ states are "reservoir" states from which emission may be neglected [15,16]. The

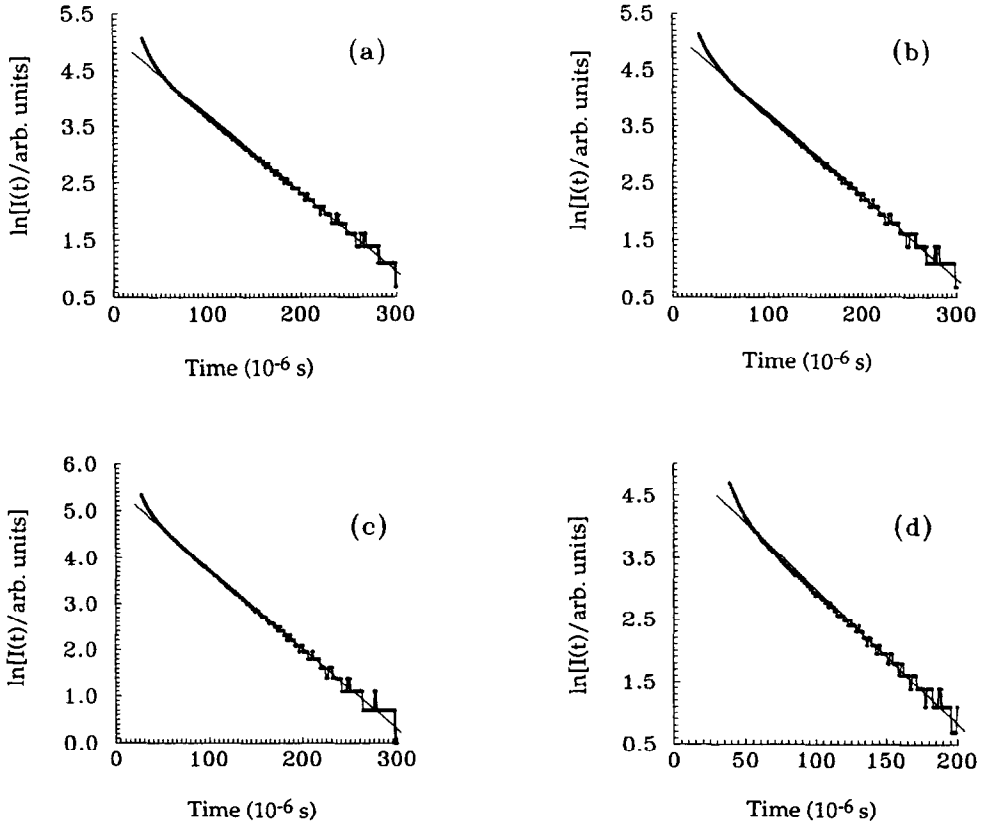

Fig. 3. Examples of the computerized fitting of the digitized output, indicating the first-order decay of the time-resolved atomic fluorescence emission $I(t)$ at $\lambda = 689.3$ nm ($Sr[5s6p(^3P_1)] \rightarrow Sr[5s^2(^5S_0)]$) following the pulsed dye-laser excitation of strontium vapour at the resonance wavelength in the presence of helium buffer gas ($p_{He} = 80$ Torr, 9.1×10^{17} atoms cm^{-3} at 850 K) at elevated temperatures. T (K): (a) 850; (b) 830; (c) 790; (d) 750.

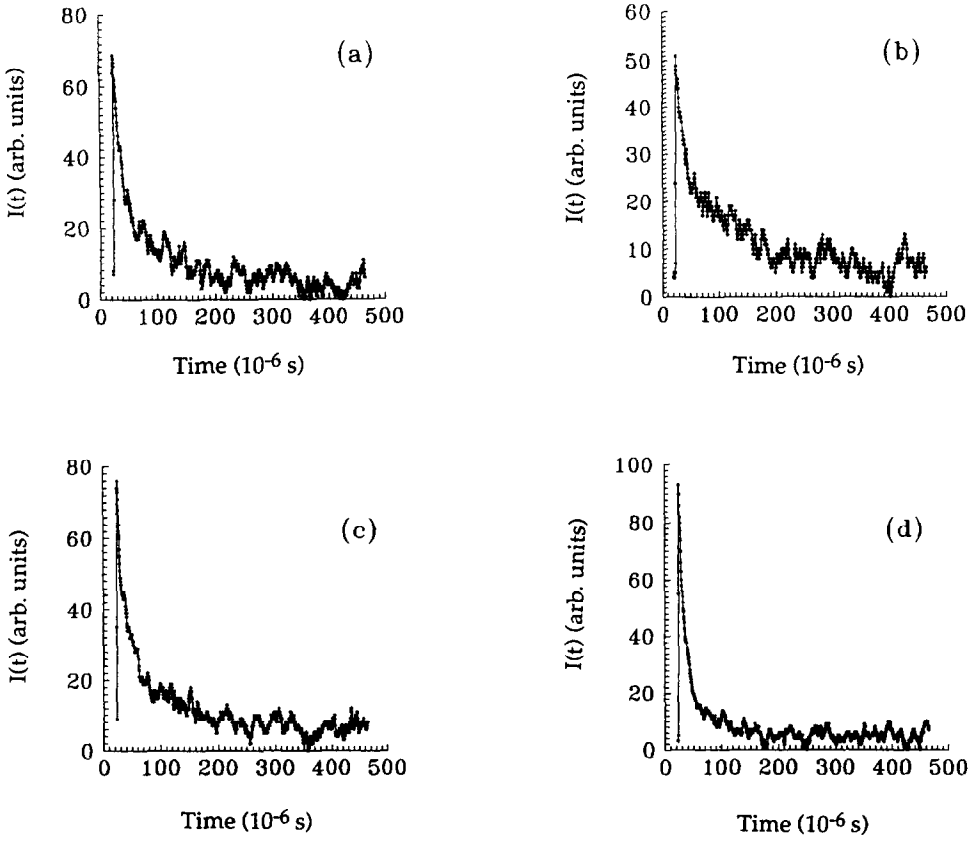

Fig. 4. Examples of the time variation of the digitized output, showing the decay of the time-resolved atomic emission $I(t)$ at $\lambda = 1124.1$ nm ($Sr[5s6s(^1S_0)] \rightarrow Sr[5s5p(^1P_1)]$), indicating energy pooling following the pulsed dye-laser excitation of strontium vapour at $\lambda = 689.3$ nm ($Sr[5s5p(^3P_1)] \leftarrow Sr[5s^2(^1S_0)]$) in the presence of helium buffer gas ($p_{He} = 80$ Torr, 9.1×10^{17} atoms cm^{-3} at 850 K) at elevated temperatures. T (K): (a) 850; (b) 830; (c) 790; (d) 750.

slopes of these first-order plots may then be recast in the standard form [15,16]

$$k' = gA_{nm}/F + \beta/p_{He} \quad (3)$$

where

$$F = 1 + 1/K_1 + K_2 \quad (4)$$

neglecting collisional quenching by He and $Sr(5^1S_0)$ ($\Sigma k_Q[Q]$), and this yields the appropriate decay coefficients in the presence of He alone. g is the "escape factor" resulting from solutions of the diffusion equation for radiation which has been demonstrated as appropriate for radiation trapping in this type of system for the transition at $\lambda = 689.3$ nm [14]. Its quantitative characterization is not required in the present measurements, but the variation in g yields the main variation in k' for the various atomic states which is necessary in this investigation. K_1 and K_2 represent the equilibrium constants connecting the spin–orbit states within $Sr(5^3P_J)$ ($^3P_0 \rightleftharpoons {}^3P_1$, K_1; $^3P_1 \rightleftharpoons {}^3P_2$, K_2) which rapidly reach Boltzmann equilibrium on the time scales of the present measurements. Emission is observed only from $Sr(5^3P_1)$ and the term β/p_{He} represents the diffusional loss of $Sr(5^3P_J)$. The function F, calculated by statistical thermodynamics, takes the value of 2.311 at $T = 850$ K, for example. The detailed time scale by which the Boltzmann equilibrium has been reached for $Sr(5^3P_J)$ in helium alone is a matter of some controversy. The application in various publications of such rapid equilibration and the standard use of the 5^3P_0 and 5^3P_2 states as "reservoir states" leads to a mean radiative lifetime of $\tau_e = 19.6_{-0.5}{}^{+0.6}$ μs [9]. Kelley et al. [6] describe time-resolved measurements on all the $Sr(5^3P_{0,1,2})$ spin–orbit states and conclude a mean radiative lifetime for $Sr(5^3P_1)$ of $\tau_e = 22 \pm 0.5$ μs which is not very different from that reported hitherto [9]. This will not significantly affect the present analysis where radiation trapping and the "escape factor" will be more important in determining the effective value of A_{nm} or τ_e. All measurements were carried out at constant total pressure, with the accompanying small contribution to atomic loss by diffusion (Eq. (3)), which is only mildly temperature dependent across the limited temperature range employed here [9].

Fig. 4 gives examples of the digitized time variation of the emission at $\lambda = 1124.1$ nm ($Sr[5s6s(^1S_0)] \rightarrow Sr[5s5p(^1P_1)]$) under identical chemical conditions to those indicated in Fig. 2, demonstrating the production of the $5s6s(^1S_0)$ state by energy pooling. The profiles are scattered, as expected for the low sensitivity of the photomultiplier tube at this wavelength; nevertheless, the pooling emission has now been observed, recorded and quantitatively characterized from the kinetic viewpoint. Fig. 4 was recorded with a

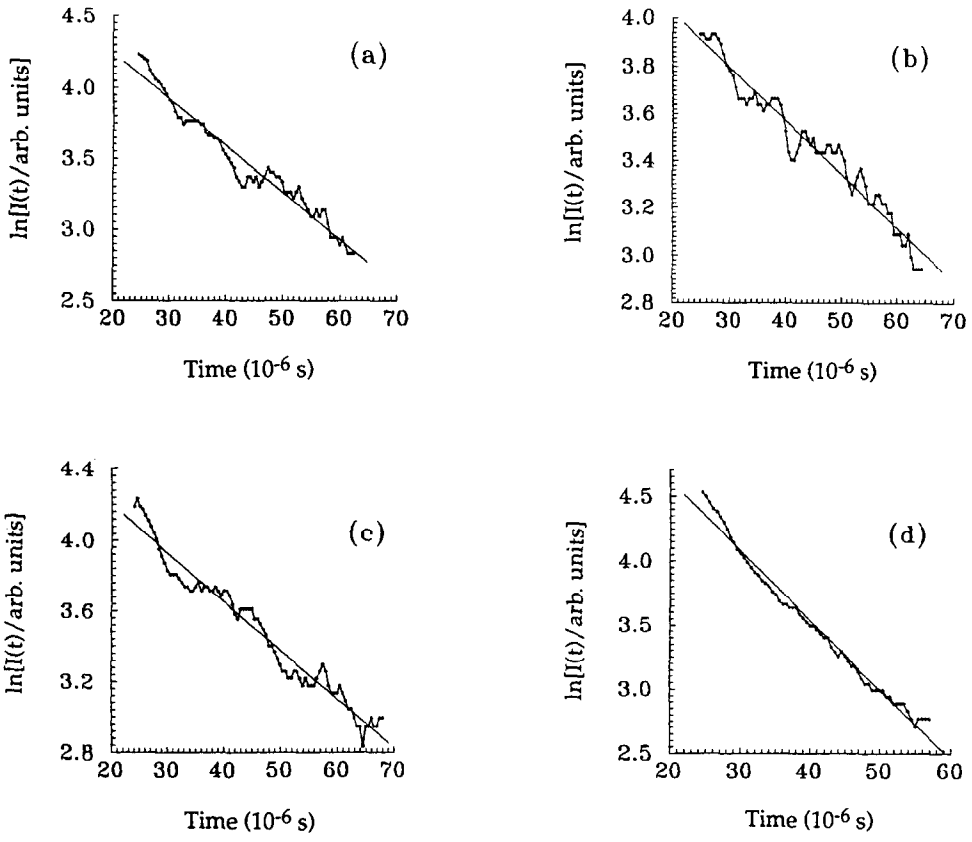

Fig. 5. Examples of the time variation of the computerized fitting of the digitized output, indicating the first-order decay of the time-resolved atomic emission $I(t)$ at $\lambda = 1124.1$ nm ($Sr[5s6s(^1S_0)] \rightarrow Sr[5s5p(^1P_1)]$) resulting from energy pooling following the pulsed dye-laser excitation of strontium vapour at $\lambda = 689.3$ nm ($Sr[5s5p(^3P_1)] \leftarrow Sr[5s^2(^1S_0)]$) in the presence of helium buffer gas ($p_{He} = 80$ Torr, 9.1×10^{17} atoms cm^{-3} at 850 K) at elevated temperatures. T (K): (a) 850; (b) 830; (c) 790; (d) 750.

photomultiplier voltage of 1200 V, in contrast with the use of 600 V in Fig. 2 for the atomic resonance transition where the gain in the photomultiplier tube has thus been increased by a factor of 357 (see Section 2) to offset the lower optical sensitivity. Fig. 5 shows the first-order plots constructed from the data in Fig. 4 and yields the first-order decay coefficients for the $5s6s(^1S_0)$ state. Fig. 6 gives examples of the digitized decay profiles for the cascading fluorescence at $\lambda = 460.7$ nm ($Sr[5s5p(^1P_1)] \rightarrow Sr[5s^2(^1S_0)]$) under identical chemical conditions to those given in Figs. 2 and 4. Here a photomultiplier voltage of 800 V was employed, indicating an increase in photomultiplier gain of 11.5 to that employed for the atomic resonance transition. The first-order decay profiles constructed for $Sr[5s5p(^1P_1)]$ for the data in Fig. 6 are given in Fig. 7.

Comparison of the first-order decay coefficients for the energy pooled state $Sr[5s6s(^1S_0)]$, obtained from plots of the type given in Fig. 5, with those for the store state $Sr[5s5p(^3P_J)]$ (Fig. 3) is given in Fig. 8(a). This yields a slope of 2.04, a factor of two within experimental error. Notwithstanding the quality of the plot, placed through the origin as this is a physically realistic point, we ascribe a 1σ error of approximately 10% in view of the scatter in the raw data. The analogous comparison of the first-order decay coefficients for the pooled state with the $5s5p(^1P_1)$ cascading state is given in Fig. 8(b) with a slope of 0.994, unity within experimental error, and a comparable 1σ error of 10%. Figs. 8(a) and 8(b) demonstrate the variation in the values of the first-order coefficients, arising initially from those for $Sr[5s5p(^3P_J)]$, obtained principally through the radiation trapping "escape factor" g.

The mechanism for the $5s6s(^1S_0)$ energy pooled states observed in this investigation following pulsed generation of $Sr(5^3P_J)$ is thus consistent with the simple mechanism of self-annihilation with strongly allowed emission at $\lambda = 1124.1$ nm. Thus the production of $Sr[5s6s(^1S_0)]$ with subsequent emission at $\lambda = 1124.1$ nm ($Sr[5s6s(^1S_0)] \rightarrow Sr[5s5p(^1P_1)] + h\nu, A_{nm}(2)$) may be written

$$Sr(5^3P_J) + Sr(5^3P_J) \longrightarrow Sr[5s6s(^1S_0)] + Sr[5s^2(^1S_0)] \qquad k_1$$

$$Sr[5s6s(^1S_0)] \longrightarrow Sr[5s5p(^1P_1)] + h\nu(\lambda = 1124.1 \text{ nm}) \qquad A_{nm}(2)$$

The rate constant k_1 has been characterized by Kelley et al. [8] for $T = 673$ K, namely $k_1 = (1.1 \pm 0.4) \times 10^{-10}$ cm^3 atom^{-1} s^{-1}. The endothermicity for the pooling process depends on the spin–orbit Boltzmann averaged energy for the ^3P_J state. Kelley et al. [8] ascribe an endothermicity (ΔE)

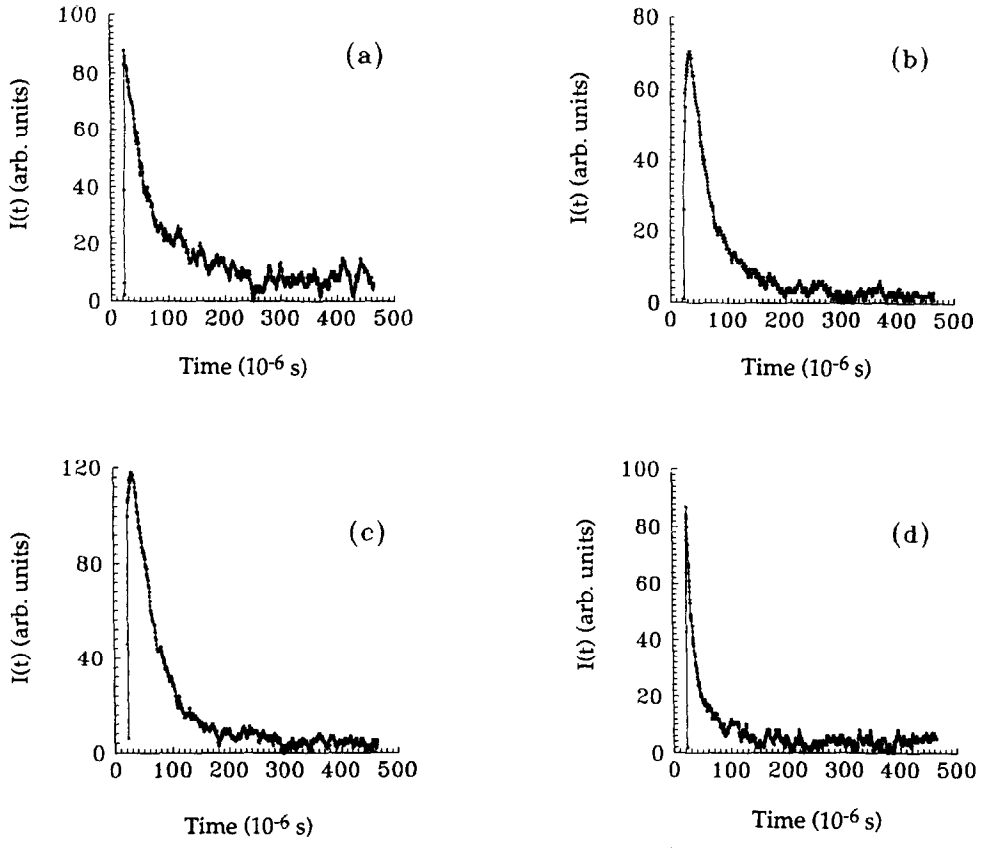

Fig. 6. Examples of the time variation of the digitized output, showing the decay of the time-resolved atomic emission $I(t)$ at $\lambda = 460.7$ nm ($Sr[5s5p(^1P_1)] \rightarrow Sr[5s^2(^1S_0)]$), indicating cascading fluorescence from energy pooling following the pulsed dye-laser excitation of strontium vapour at $\lambda = 689.3$ nm ($Sr[5s5p(^3P_1)] \leftarrow Sr[5s^2(^1S_0)]$) in the presence of helium buffer gas ($p_{He} = 80$ Torr, 9.1×10^{17} atoms cm^{-3} at 850 K) at elevated temperatures. T (K): (a) 850; (b) 830; (c) 790; (d) 750.

of $+1583$ cm^{-1}, which would correspond to a Boltzmann factor ($\exp(-\Delta E/kT)$) of 3.3×10^{-2}. The collision number for the process described by k_1 must therefore be approximately 3.3×10^{-9} cm^3 atom^{-1} s^{-1} which is large. The concentration of $Sr[5s6s(^1S_0)]$ is placed in steady state and the emission intensity at $\lambda = 1124.1$ nm is thus given by

$$I_{nm}(1124.1\text{ nm}) = GSk_1[Sr(5s5p(^3P_J)]_{t=0}{}^2 \exp(-k't) \quad (5)$$

following Eq. (1). Hence the first-order decay coefficient for the pooled state is double that of the $Sr(5^3P_J)$ store state. G is the gain of the photomultiplier, which is a function of voltage, and S is the sensitivity of the optical system as a function of wavelength, the calibration of which have been given in Section 2. Mechanistically, the emission at $\lambda = 460.7$ nm from $Sr[5s5p(^1P_1)]$ ($Sr[5s5p(^1P_1)] \rightarrow Sr[5s^2(^1S_0)] + h\nu$, $A_{nm}(3) = 2.01 \times 10^8$ s^{-1} [16–19]) demonstrates the same time-dependent behaviour.

The optical calibration may be coupled with the atomic emission intensities at $\lambda = 460.7$ nm (Fig. 6) and $\lambda = 1124.1$ nm (Fig. 4) using the photomultiplier gain characteristic (see Section 2) to estimate the Einstein A coefficient for the latter. This may be determined, for example, from the measurement of the ratio of the integrated intensities from the profiles of Figs. 4(a) and 6(a). Such measurements for suitable combinations of intensities taken under identical conditions were repeated across the range of temperature employed here. The result, of course, depends on the value employed for $A_{nm}(3)$ for emission from the $5s5p(^1P_1)$ state and assuming that all the emission at $\lambda = 460.7$ nm is cascading fluorescence and originates from $Sr[5s6s(^1S_0)]$ via energy pooling. Using $A_{nm}(3) = 2.01 \times 10^8$ s^{-1} [19], the results yield $A_{nm}(2)(\lambda = 1124.1\text{ nm}) = 7.2 \times 10^8$ s^{-1}. Using the earlier value of $A_{nm}(3) = 2.83 \times 10^7$ s^{-1} [15], we obtain $A_{nm}(2) = 1.01 \times 10^8$ s^{-1}. Whilst we may confidently employ the time profiles in Fig. 4, and hence Fig. 5, to characterize the first-order decay coefficients for $Sr[5s6s(^1S_0)]$ with reasonable accuracy, the intensity measurements are subject to large errors both on account of the low sensitivity at the long wavelength and the response of the grating in the monochromator (Fig. 1). Accordingly, we conclude that $A_{nm}(2)(\lambda = 1124.1\text{ nm}) \approx 10^8$ s^{-1}, further justifying the steady state mechanism for $Sr[5s6s(^1S_0)]$ leading to Eq. (5).

Finally, we may note the feasibility of further applications of the novel optical detection system to studies of emission from low-lying electronically excited states of various atoms (or molecules). A long-wavelength limit of approximately 1200 nm indicates that studies of time-resolved emission from electronically excited atoms at energies greater than about 1.03 eV above the ground state are, in principle, accessible. In the present context of electronically excited alkaline

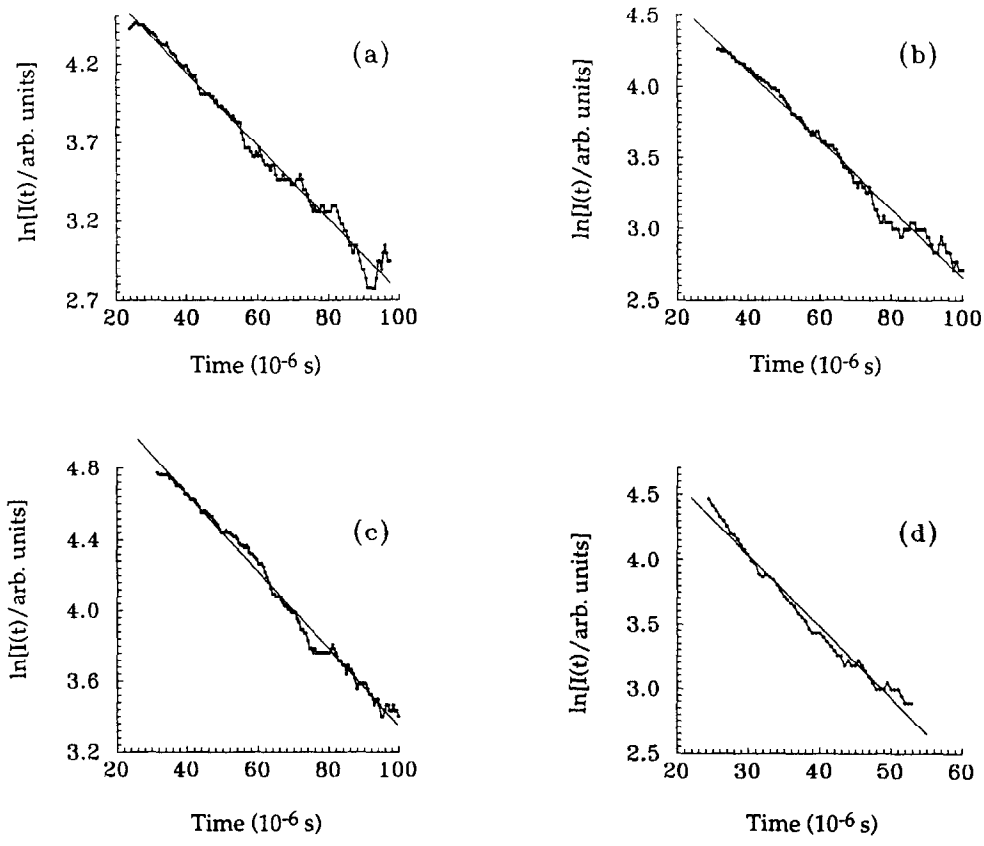

Fig. 7. Examples of the time variation of the computerized fitting of the digitized output, indicating the first-order decay of the time-resolved atomic emission $I(t)$ at $\lambda = 460.7$ nm ($Sr[5s5p(^1P_1)] \rightarrow Sr[5s^2(^1S_0)]$) for the cascading fluorescence from energy pooling following the pulsed dye-laser excitation of strontium vapour at $\lambda = 689.3$ nm ($Sr[5s5p(^3P_1)] \leftarrow Sr[5s^2(^1S_0)]$) in the presence of helium buffer gas ($p_{He} = 80$ Torr, 9.1×10^{17} atoms cm^{-3} at 850 K) at elevated temperatures. T (K): (a) 850; (b) 830; (c) 790; (d) 750.

earth atoms, direct studies on $Ba[6s5d(^3D_{1,2,3})]$ (1.120, 1.143 and 1.190 eV respectively) and $Ba[6s5d(^1D_2)]$ (1.413 eV) [7] in emission should be feasible. Estimates of the mean radiative lifetimes of such states [4] indicate that they are sufficiently metastable to be investigated in the present system [20–22]. Eversole and Djeu [22] have studied the time-dependent behaviour of $Ba[6s5d(^1D_2)]$ by atomic resonance absorption to the $5d6p(^1P_1^o)$ state at $\lambda = 582.6$ nm. Time-resolved emission from the optically metastable states generally enjoys the advantage that the emission itself constitutes its own spectroscopic marker with standard electronic methods, without a second optical source for absorption or fluorescence monitoring, and permits accompanying emission studies for other states to be carried out at constant light

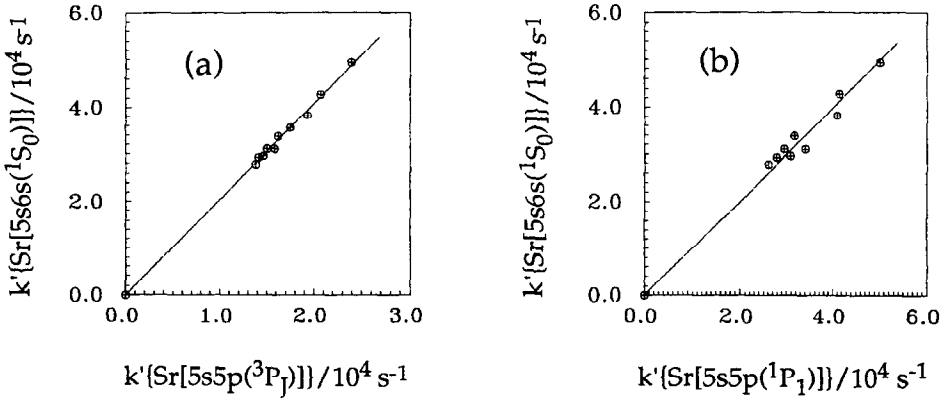

Fig. 8. (a) Comparison of the first-order rate coefficients k' derived from the intensity profiles for the emission of the energy pooled state ($Sr[5s6s(^1S_0)] \rightarrow Sr[5s5p(^1P_1)]$) at $\lambda = 1124.1$ nm with that for the atomic emission at $\lambda = 689.3$ nm ($Sr[5s5p(^3P_1)] \rightarrow Sr[5s^2(^1S_0)]$) (slope = 2.04). (b) Analogous comparison of the first-order decay coefficients for the pooled state ($Sr[5s6s(^1S_0)] \rightarrow Sr[5s5p(^1P_1)]$) at $\lambda = 1124.1$ nm with the cascading emission ($Sr[5s5p(^1P_1)] \rightarrow Sr[5s^2(^1S_0)]$) at $\lambda = 460.7$ nm (slope = 0.994). (Following pulsed dye-laser excitation of strontium vapour at the resonance wavelength in the presence of excess helium buffer gas at elevated temperatures ($T = 750$–890 K).)

gathering power of the optical system as in the present investigation on atomic strontium.

Acknowledgements

We thank the Cambridge Overseas Scholarship Trustees for a Research Studentship held by J.L. during the tenure of which this work was carried out. J.L also thanks the ORS for an award. We also thank the EPSRC of Great Britain for the initial purchase of the laser system and a Research Studentship held by one of us (S.A.). Finally, we are also indebted to Dr. George Jones of the DRA (Fort Halstead) for encouragement and helpful discussions.

References

[1] W.H. Breckenridge and H. Umemoto, *Adv. Chem. Phys., 50* (1982) 325.
[2] W.H. Breckenridge, in A. Fontijn and M.A.A. Clyne (eds.), *Reactions of Small Transient Species: Kinetics and Energetics*, Academic Press, London, Chapter 4, p. 157.
[3] D. Husain and G. Roberts, in M.N.R. Ashfold and J.E. Baggott (eds.), *Bimolecular Collisions: Advances in Gas Phase Photochemistry and Kinetics*, The Royal Society of Chemistry, London, 1989, Chapter 6, p. 263.
[4] D. Husain, *J. Chem. Soc., Faraday Trans. 2, 85* (1989) 85.
[5] P.J. Dagdigian and M.L. Campbell, *Chem. Rev., 87* (1987) 1.
[6] J.F. Kelley, M. Harris and A. Gallagher, *Phys. Rev. A, 37* (1988) 2354.
[7] C.E. Moore (ed.), *Atomic Energy Levels, Nat. Bur. Stand. (U.S.) Ref. Data Ser. 35*, Vols. I and II, US Government Printing Office, Washington DC, 1971.
[8] J.F. Kelley, M. Harris and A. Gallagher, *Phys. Rev. A, 38* (1988) 1225.
[9] D. Husain and G. Roberts, *Chem. Phys., 127* (1988) 203.
[10] D. Husain and J. Lei, *J. Chem. Soc., Faraday Trans., 91* (1995) 811.
[11] S. Antrobus, S.A. Carl, D. Husain, J. Lei, F. Castaño and M.N. Sanchez Rayo, *Ber. Bunsenges. Phys. Chem., 99* (1995) 127.
[12] S. Antrobus, D. Husain, J. Lei, F. Castaño and M.N. Sanchez Rayo, *Int. J. Chem. Kinet.*, in press.
[13] D.R. Lide and H.P.R. Frederiske (eds.), *CRC Handbook of Physics and Chemistry*, CRC Press, Boca Raton, FL, 75th edn., 1994, pp. 4–124.
[14] D. Husain and J. Lei, *J. Photochem. Photobiol. A: Chem., 87* (1995) 89.
[15] C.H. Corliss and W.R. Bozmann, *Experimental Transition Probabilities for Spectral Lines of Seventy Elements, Nat. Bur. Stand. (U.S.) Monograph 53*, US Government Printing Office, Washington DC, 1962, pp. 388–389.
[16] J. Reader, C.H. Corliss, W.L. Wiese and G.A. Martin, *Wavelengths and Transition Probabilities for Atoms and Atomic Ions, Nat. Bur. Stand. (U.S.) Ref. Data Series NSRDS-NBS-68*, US Government Printing Office, Washington DC, 1980, p. 398.
[17] J. Migdalek and W.E. Baylis, *Can. J. Phys., 65* (1987) 1612.
[18] F.M. Kelley and M.S. Mathur, *Can. J. Phys., 58* (1980) 1416.
[19] D.R. Lide and H.P.R. Frederiske (eds.), *CRC Handbook of Physics and Chemistry*, CRC Press, Boca Raton, FL, 75th edn., 1994, pp. 10–170.
[20] R.W. Solarz and S.A. Johnson, *J. Chem. Phys., 70* (1979) 3592.
[21] S.G. Schmelling, *Phys. Rev. A, 9* (1974) 1097.
[22] J.D. Eversole and N. Djeu, *J. Chem. Phys., 71* (1979) 148.